Biochemical and Biophysical Research Communications 458 (2015) 14–20

Contents lists available at ScienceDirect

Biochemical and Biophysical Research Communications

journal homepage: www.elsevier.com/locate/ybbrc

HIF-1α suppressing small molecule, LW6, inhibits cancer cell growth by binding to calcineurin b homologous protein 1

Beom Seok Kim [a, 1], Kyeong Lee [b, 1], Hye Jin Jung [c], Deepak Bhattarai [b], Ho Jeong Kwon [a, d, *]

[a] Chemical Genomics National Research Laboratory, Department of Biotechnology, Translational Research Center for Protein Function Control, College of Life Science and Biotechnology, Yonsei University, Seoul 120-752, Republic of Korea
[b] College of Pharmacy, Dongguk University-Seoul, Goyang 410-820, Republic of Korea
[c] Department of Pharmaceutical Engineering, SunMoon University, #100, Kalsan-ri, Tangjeong-myeon, Asan-si, Chungnam 336-708, Republic of Korea
[d] Department of Internal Medicine, Yonsei University College of Medicine, Seoul 120-752, Republic of Korea

ARTICLE INFO

Article history:
Received 6 January 2015
Available online 17 January 2015

Keywords:
Angiogenesis
Calcineurin b homologous protein 1
Hypoxia-inducible factor-1α
LW6
Target identification

ABSTRACT

Hypoxia inducible factor-1 alpha (HIF-1α) plays an important role in angiogenesis and metastasis and is a promising therapeutic target for the development of anti-cancer drugs. We recently developed a new synthetic small molecule inhibitor of HIF-1α, LW6, which results in inhibition of angiogenesis. To investigate its underlying mechanism, target protein identification was conducted by reverse chemical proteomics using phage display. We identified calcineurin b homologous protein 1 (CHP1) as a target protein of LW6, which specifically binds to CHP1 in a Ca^{2+} dependent manner. Covalent labeling of LW6 using photoaffinity and click chemistry demonstrated its co-localization with CHP1 in live cells. HIF-1α was decreased by CHP1 knockdown in HepG2 cells, and angiogenesis was not induced in HUVEC cells by treatment with conditioned media from CHP1 knockdown cells compared to the control. These data demonstrated that LW6 inhibited HIF-1α stability via direct binding with CHP1 resulting in suppression of angiogenesis, providing a new insight into the role of CHP1 in HIF-1α regulation. LW6 could serve as a new chemical probe to explore CHP1 function.

1. Introduction

Hypoxia is the environmental condition of the absence of oxygen. It is a key feature of most tumor environments contributing to chemoresistance, radioresistance, angiogenesis, metastasis, resistance to cell death, and altered genomic instability and metabolism [1]. Hypoxia inducible factor (HIF) is a key transcriptional factor responsible for tumorigenesis inducing drug-resistance and angiogenesis; therefore, numerous drug discovery efforts targeting HIF-1α are currently ongoing. For example, phenethylisothiocyanate and Acriflavine [2] are under investigation as anti-cancer drugs [3–5]. HIF-1α also plays an important role in angiogenesis [6]. We have previously developed several inhibitors of HIF-1α stability from synthetic libraries harboring hydrophobic moiety of adamantyl-ring structure and have evaluated their biological activities.

Among the characterized inhibitory compounds, LW6 showed the most potent inhibitory activities against HIF-1α stability by up-regulation of VHL inducing HIF-1α degradation [7]. Recently, malate dehydrogenase 2 (MDH2) was identified as one of the target proteins of LW6 using activity-based chemical probes in HCT116 cells [8]. Simultaneously, we attempted to identify additional, new LW6 target proteins using affinity-based phage display cloning from human cDNA libraries [9] to elucidate the underlying mechanisms responsible for the suppressive activity of LW6 on HIF-1α stability. Conventionally, “one drug-single target” has been the general concept with respect to target identification for small molecules. Recently, however, owing to development of multi-omics technologies, “one drug-multiple targets; single pharmacological effect” has been recognized as a biologically relevant paradigm for the mode of action of small molecules. For instance, protein kinase inhibitors such as sorafenib and sunitinib were

Abbreviations: CHP1, calcineurin b homologous protein 1; FBS, fetal bovine serum; HIF-α, hypoxia inducible factor-1 alpha; HUVEC, human umbilical vein endothelial cell; MTT, 3-(4,5-dimethylthiazol-2-yl)-2,5-diphenyl tetrazolium bromide; siRNA, small interfering RNA; SPR, surface plasmon resonance; K_D, dissociation constant.

* Corresponding author. Department of Internal Medicine, Yonsei University College of Medicine, Seoul 120-752, Republic of Korea. Fax: +82 2 362 7265.
E-mail address: kwonhj@yonsei.ac.kr (H.J. Kwon).

[1] These authors contributed equally to this work.

http://dx.doi.org/10.1016/j.bbrc.2015.01.031
0006-291X/

approved as anti-cancer drugs for their inhibition of multiple kinases [10].

In this study, we identify calcineurin b homologous protein 1 (CHP1) as a new target protein of LW6, highlighting CHP1 in the regulation of HIF-1α. Furthermore, these results demonstrate that CHP1 could be a new means by which to control HIF-1α activity for inhibition of cancer cell growth and eventually suppression of angiogenesis.

2. Materials and methods

2.1. Materials

EBM-2 was purchased from Lonza (San Diego, CA), and fetal bovine serum (FBS) was from Invitrogen (Grand Island, NY). Matrigel™ was obtained from BD Biosciences (Bedford, MA). Transwell plates were from Corning Costar (Cambridge, MA). DMEM and streptoavidin (SA) sensor chips were purchased from Thermo Fisher Scientific (Waltham, MA).

2.2. Chemistry

Synthesis of LW6, Biotinyl-LW6, and the LW6 derived multifunctional probe (1) were prepared following the previously reported procedures [6].

2.3. Cell culture and proliferation assay

HepG2, HUH7, and Hep3B cells were maintained at 37 °C under a humidified atmosphere of 5% CO_2 in DMEM medium supplemented with 10% FBS and 1% antibiotics. For detection of HIF-1α, HepG2 cells were seeded at a density of 2×10^5 cells/mL/well in a 6-well plate at 37 °C for 20 h for subsequent experiments. After treatment of LW6 for 1 h, hypoxic stimulation of the cells was induced by replacing cell atmosphere with 5% CO_2, 10% H_2, and 85% N_2 in a hypoxia chamber for 4 h.

Proliferation was measured using 3-(4,5-dimethylthiazol-2-yl)-2,5-diphenyl tetrazolium bromide (MTT; Sigma–Aldrich, Saint Louis, MO), and cellular morphology was observed using an Olympus IX70 microscope at 100X magnification (Olympus America, Inc., Melville, NY). Independent experiments were repeated at least three times.

2.4. Phage display biopanning

Biotinyl-LW6 diluted in Tris-buffered saline (TBS [pH 7.5]) was immobilized onto a streptoavidin-coated well (Pierce Biotechnology, Inc.) at a 10 μM concentration for 1 h. T7 phage particles encoding human cDNA libraries from liver tumor tissues (Novagen, Madison, WI) were diluted in TBS (8×10^8 pfu/mL) and added to the LW6-immobilized wells. After incubation for 1 h, the well plate was washed ten times with TBS. The final wash solutions were collected as wash samples and LW6 bound phage particles were eluted for 1.5 h with 100 μM LW6 free compound diluted in TBS. The eluted phage particles were amplified after infection into *Escherichia coli* strain BLT5615, and amplified phage particles were utilized for next round biopanning. After 10th round biopanning, eluted phages were infected into BLT5615 grown on an LB agar ampicillin plate (50 μg/mL). The plaques formed on the agar plate were isolated, and cDNA fragments from the isolated plaques were sequenced by Macrogen Inc. (Seoul, Korea).

2.5. SPR analysis

Biotinyl-LW6 diluted in BIAcore running buffer (pH7.4, 10 mM HEPES, 150 mM NaCl) without EDTA was immobilized on the surface of a streptoavidin-coated sensor chip at a concentration of 200 μM. Before injection of CHP1, the surface of the sensor chip with immobilized biotinyl-LW6 was harshly washed by 50 mM NaOH diluted in BIAcore buffer for 2 min at a 5 μL/min flow rate. Purified bovine brain CHP1 (Enzo Life Science Inc., Farmingdale, NY) was flowed through the biotinyl-LW6 immobilized streptoavidin sensor chip at the desired concentration for 2 min (flow rate: 30 μL/min). Association and dissociation curves were obtained on a BIAcore 2000. The surface of the sensor chip was regenerated by injection of 10 μL regeneration buffer (10 mM NaCl and 10 mM NaOH). SPR response curves were analyzed with BIAcore evaluation software, version 3.1. The apparent dissociation constants were calculated from the kinetic constant: $K_D = kd/ka^*$.

2.6. Western blot analysis

Cell lysates were separated by 10% sodium dodecyl sulfate polyacrylamide gel electrophoresis and transferred to polyvinylidenefluoride membranes (Millipore, Bedford, MA) using electroblotting procedures. Blots were blocked and immunolabeled overnight at 4 °C with primary antibodies, including anti- HIF1- α (BD Bioscience, Franklin Lakes, NJ), anti-CHP1 (Novus Biologicals, Littleton, CO), anti-malate dehydrogenase 2 (Cell Signaling Technology, Danvers, MA), anti-tubulin (Milipore, Billerica, MA), and anti-beta actin (Abcam, Cambridge, MA), antibodies. Immunolabeling was detected using an enhanced chemiluminescence kit (Thermo Fisher Scientific).

2.7. Click chemistry in cells and imaging

HepG2 cells were plated on 6-well plates (1×10^4 cells) containing glass coverslips and incubated at 37 °C for 24 h. After treatment of LW6 derived photoaffinity probes with trifluorodiazirine for 1 h, cells were washed 3 times with PBS and irradiated by 365 nm UV for 30 min. Then, cells were washed again with PBS fixed with 4% paraformaldehyde in PBS for 5 min. After washing with PBS, cells were permeabilized with 0.2% Triton X-100 in PBS for 5 min, blocked with 1% BSA in PBS for 10 min, and then CHP1 primary antibody was applied for 1 h. After washing with PBS, the secondary antibody (Alexa Flour-594 rabbit; Invitrogen) was applied, and the click reaction was performed with the Click-iT Cell Reaction Buffer Kit (Invitrogen) according to the manufacturer's instructions for 1 h. Finally, cells were washed three times with PBS and analyzed by confocal microscopy (Carl Zeiss, Oberkochen, Germany).

2.8. siRNA transfection for CHP1 knockdown

HepG2 cells were seeded onto 6-well plates and incubated for 16 h at 37 °C under a humidified atmosphere of 5% CO_2 in DMEM medium supplemented with 10% FBS and 1% antibiotics. CHP1 siRNA (Thermo Fisher Scientific) was transfected into the cells using Lipofetamine RNAiMax (Thermo Fisher Scientific) for 24 h according to the manufacturer's instructions.

2.9. Docking model of LW6-CHP1

A docking study was performed using the Surflex-Dock program from Tripos (Princeton, NJ) with the SYBYL module. For CHP1 target (pdb code:2ct9), docking with LW6 or its probe generally showed a good score. The binging mode was calculated using the Surflex-

Dock score (Total_Score, Crash, and Polar). In addition, the D score, PMF score, G score, and ChemScore were also calculated.

2.10. Statistical analysis

All results represent mean ± standard deviation of three independent experiments. Student's t-test was used to determine statistically significant differences between the control and test groups. A p value less than 0.05 was considered significant.

3. Results

3.1. Identification of CHP1 as a binding protein of LW6 by phage display biopanning

Biotinyl-LW6 was synthesized for the immobilization of the compound on a streptavidin solid surface (Fig. 1A). The biological activity of biotinyl-LW6 was assessed through its inhibitory activity against HIF-1α stability. Biotinyl-LW6 induced degradation of HIF-1α in HepG2 cells with an IC_{50} of 10 μM, which is 2-fold weaker than that of LW6 but which still indicates biological activity (Fig. 1B). Biotinyl-LW6 was subsequently immobilized onto streptavidin-coated wells, and T7 phages encoding human cDNA libraries from liver tumors were combined and applied for affinity based selection using the LW6 binding protein. Phage plaques bound to LW6 increased in proportion to each round of biopanning, implying that specific LW6 binding phages were enriched after the process of biopanning rounds (Fig. 1C and Fig. S1). Tenth-round phages were isolated and analyzed by DNA sequencing using a plaque forming assay as described previously. A total of 24 phage plaques were isolated for sequence analysis. The amino acids sequences expressed by each phage were determined via homology analysis using BLAST search. Among the 24 phage plaques isolated, 14 were identified as calcineurin b homologous protein1 (CHP1)-coding phages (approximately 46% of the total isolated phage clones) and 9 represented calmodulin (CaM)-coding phages (30%) (Table S1). One clone was determined to be the nuclear pre-ribosomal associated protein 1 (100% identity), which were revealed as a nonspecific binder through phage binding assays (Fig. S2).

Interestingly, both of the highly represented protein coding phages bound to LW6, CaM and CHP1, are calcium binding proteins (Fig. S2). We selected CHP1 as the LW6 target protein for the following study, as CaM is a well-known protein involved in HIF-1α

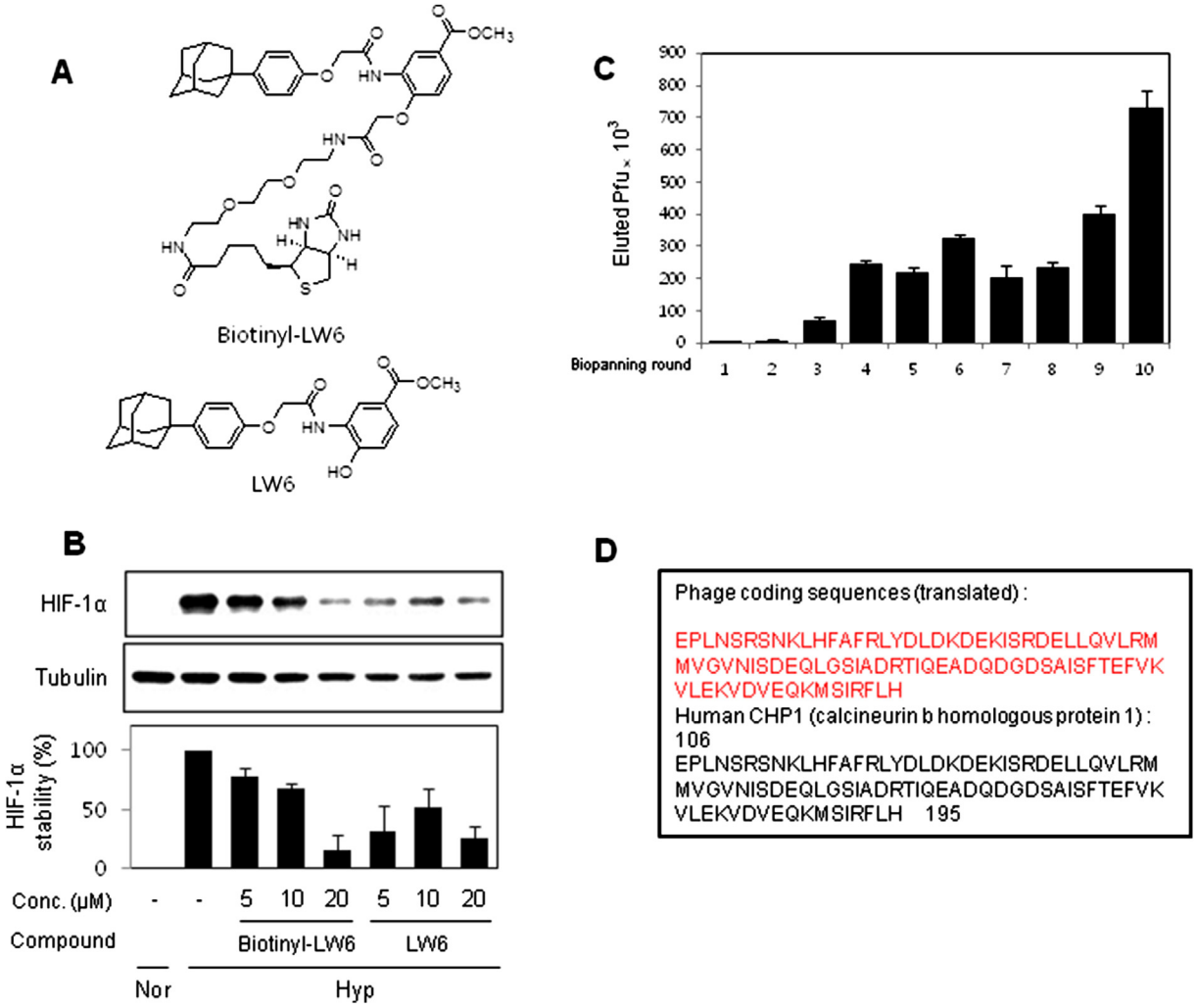

Fig. 1. Identification of LW6 binding proteins using phage display biopanning. (A) The structure of LW6 and its molecular probe (biotinyl-LW6) are shown. Biotinylation of the compound was executed at the position of phenolic hydroxyl group of LW6. (B) Effects of LW6 and biotinyl-LW6 on HIF-1α stability in HepG2 cells. Western blot analysis was performed to evaluate the biological activity of the compounds. Nor: normoxia, Hyp: hypoxia (C) Analysis of LW6 binding phage numbers eluted after each round of biopanning. Pfu: plaque forming unit. (D) Amino acid sequence homology between human CHP1 and the protein from the LW6 binding phage. Phage sequences were 100% identical to the C-terminus (106–195) of human CHP1. The values represented by the error bars (means ± standard deviation).

regulation and tumor angiogenesis [11–14]. Its identification, however, validates our strategy for identifying functionally relevant LW6 target proteins.

CHP1 is a 22 kDa calcium binding protein that interacts with sodium hydrogen exchangers (NHEs) and plays a crucial role in maintenance of the intracellular ionic environment required for homeostasis [15]. However, the relationship between CHP1 and tumorigenesis has not yet been revealed. Sequence analysis verified that two different types of CHP1-coding phages were isolated (Table S1). All included the sequences encoding both the conserved EF-hand motif and the Ca^{2+} binding regions, which are essential for biological activity of CHP1. Among the two different CHP1-phage classes, we selected the first for the following study as its sequence mostly encompassed that of human CHP1, and was 100% identical to the human CHP1 C-terminal fragment (106–195) (Fig. 1D).

3.2. LW6 interacts with CHP1 in Ca^{2+}-dependent manner

To undergo the conformational change from closed to open forms, proteins contain an EF-hand domain with Ca^{2+} binding regions. The coding sequence of the isolated CHP1 contained the two EF-hand superfamily domains including the Ca^{2+} binding regions that were similar to the amino acid properties of the original CHP1 protein, which provide the secondary structure folds necessary for interaction with LW6 (Tables S2 and S3). To address whether the CHP1-phage yielded the appropriate folding to achieve the binding capability for LW6 to act as a CHP1 ligand, we conducted a phage binding assay. CHP1 expressing-phages binding to immobilized-LW6 was markedly enhamced compared to biotin, as shown in Fig. 2A. These data demonstrated that LW6 specifically bound to the CHP1 protein.

Ca^{2+} is a critical cofactor of CHP1, inducing conformational changes of CHP1 after binding to its EF-hand motifs [16]. These changes allow interaction with several CHP1 client proteins and antagonists [17]. Therefore, we investigated whether Ca^{2+} was required for the interaction between CHP1 and immobilized LW6. In the absence of the cation chelator ethylene glycol-bis (β-aminoethylether)-tetraacetic acid (EGTA), the CHP1-phage showed high affinity to immobilized LW6, whereas in the presence of EGTA, the binding affinity was dramatically decreased to that of the biotin control (Fig. 2A). In addition, exogenous addition of Ca^{2+} increased the relative binding of CHP1-phage to immobilized LW6 (Fig. 2B). To exclude the possibility that EGTA itself inhibited the binding between LW6 and CHP1, EGTA was treated with an excess amount of Ca^{2+} in the LW6-CHP1 phage binding assay (Fig. 2C). An excess amount of Ca^{2+} (5 mM) fully reversed the EGTA (2 mM)-induced disruption of the binding between LW6 and CHP1. Furthermore, surface plasmon resonance (BIAcore) (SPR) analysis was conducted to examine the direct binding interaction between LW6 and intact CHP1. Human recombinant CHP1 was immobilized on a surface of a streptavidin-coated BIAcore sensor chip, and various concentrations (0.25–5 μM) of LW6 were injected into the sensor cells to monitor the interaction between the two molecules. In the BIAcore sensorgram, resonance curves exhibited strong binding patterns from the interaction between the two molecules after the injection of CHP1 with exogenous Ca^{2+} in a dose-dependent manner, but not in the case of the bovine serum albumin (BSA) control (Fig. 2D). In addition, the binding affinity was higher than that without Ca^{2+} (Fig. 2D). The kinetic parameters (K_D) were 7.31×10^{-7} M as determined by BIAcore evaluation software, which is lower than the K_D (1.58×10^{-6} M) in the absence of Ca^{2+}. These data suggested that Ca^{2+} is an important factor for LW6 binding to CHP1.

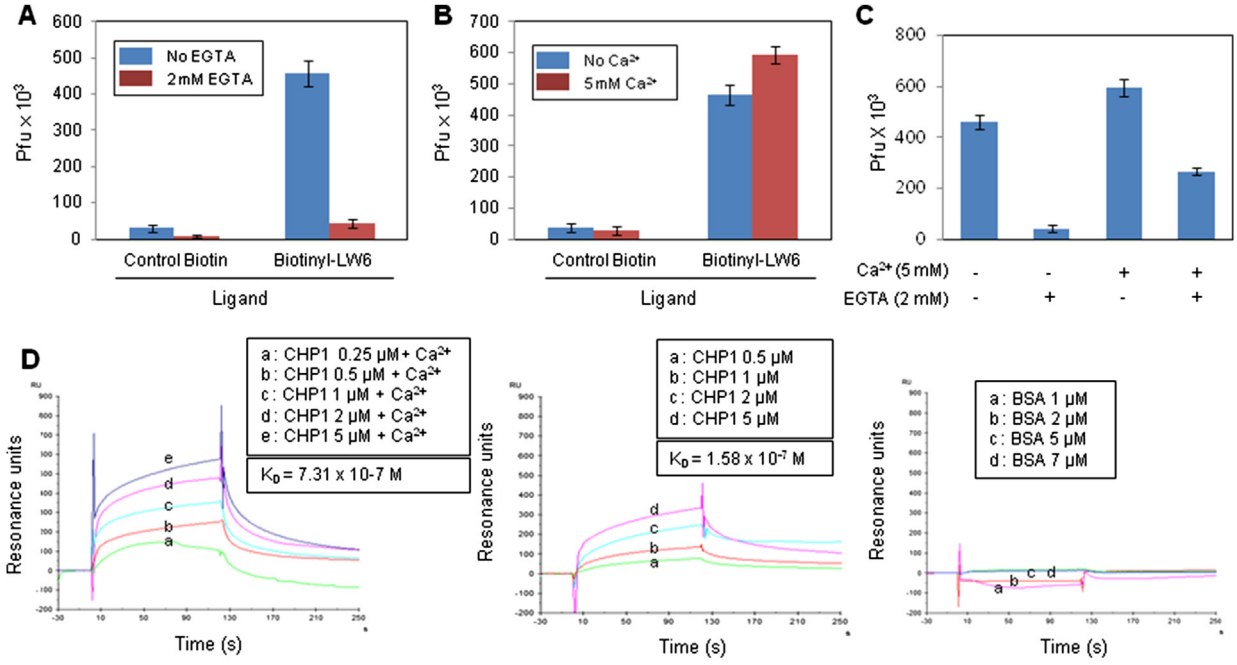

Fig. 2. LW6 specifically interacts with CHP1 in a calcium-dependent manner. (A) The effect of EGTA on the binding of the CHP1-phage to LW6. $p < 0.0002$ versus no Ca^{2+} treatment control. (B) The effect of Ca^{2+} on CHP1-phage binding to LW6. (C) Ca^{2+} is a co-factor of CHP1 for CHP1-phage binding to LW6. Inhibition of the interaction between CHP1 and LW6 by EGTA was attenuated by additional Ca^{2+} treatment, which demonstrated that Ca^{2+} is required for binding. (D) Biophysical analysis of the binding between LW6 and CHP1 using BIAcore. Biotinyl-LW6 was immobilized on a streptoavidin sensor chip, and 0.25–5 μM of purified CHP1 was loaded with (left) or without (center) Ca^{2+} onto the sensor cell. Bovine serum albumin (BSA) was used as a negative control (right). Binding sensorgrams were obtained from the BIAcore evaluation software. Dissociation constant (KD) is calculated as shown. The values represented by the error bars (means ± standard deviation).

3.3. Co-localization of LW6 and CHP1 in the cells using click chemistry and in silico docking analysis

To further validate the interaction of LW6 with CHP1 in live cells, we utilized LW6 derived probes with photoaffinity labeling and click conjugation (1; Fig. 3A). A diazirine based photoaffinity probe was generated to make a covalent bond with the peripheral amino acids using nucleophiles of the protein upon UV irradiation [18]. Probe 1 was utilized to investigate whether LW6 bound to CHP1 in the live cells via formation of a covalent bond between LW6 and CHP1. Probe 1 was labeled with Alexa Fluor-488 azide by click conjugation and CHP1 was stained with an Alexa Fluor-594 conjugated anti-rabbit secondary antibody. Probe 1 demonstrated co-localization with CHP1 in cells (Fig. 3B). Collectively, these data strongly demonstrated that LW6 interacted with CHP1 directly in live cells.

In addition, an automated docking study was performed using the Surflex Dock software program to investigate possible binding modes of LW6 in the hydrophobic pocket of CHP1 [19]. The reference protein applied to the docking system was taken from the crystal structure of CHP1 (protein data bank (PDB) entry: 2CT9). As shown in Fig. 3C, the docking results showed that LW6 fits nicely into the hydrophobic pocket of CHP1. The adamantyl-ring moiety of LW6 is located in the deep pocket of CHP1, which anchors the compound. Hydrophobic interactions between the middle chain of the LW6 and Phe176 of CHP1 stabilizes their binding along with polar interactions at CHP1 Glu162. In addition, two benzene rings linked by an LW6 amide bond might play a significant role as a capping group and thus produce more stable hydrophobic interactions with amino acids on the surface of the protein (Fig. 3C). These data strongly validated that CHP1 is a direct binding protein of LW6.

3.4. LW6 inhibits angiogenesis by perturbing CHP1

Drug susceptibility is moderated by genetic background, which mediates target protein overexpression or depletion. These differences can be utilized for target identification and validation of bioactive small molecules [20]. To address whether CHP1 expression levels affected drug sensitivity, LW6 was administered to three hepatoma cell lines, HepG2, HUH7, and Hep3B, which were selected based on CHP1 expression levels reported by the Protein Altas (http://www.proteinatlas.org). In the CHP1 overexpression lines HepG2 and HUH7, LW6 exhibited stronger anti-proliferative activity than in the other cells tested (Fig. 4A and B). These data further validated that CHP1 is a direct binding protein of LW6 in biological systems. We next investigated the effect of CHP1 knockdown on angiogenesis. CHP1 siRNA was transfected into HepG2 cells, which resulted in efficient suppression of CHP1 expression at 20 nM siRNA concentration. HIF-1α was destabilized by CHP1 genetic knockdown, which phenocopies the result following treatment with LW6 (Fig. S3 and Fig. 1B). To investigate the effects on angiogenesis, conditioned media from each knockdown cell line was applied onto human umbilical vein endothelial cells (HUVECs). We found that conditioned media from CHP1 knockdown cells did not induce tube formation and invasion of endothelial cells as compared to the control (Fig. 4C). These data demonstrated that HIF-1α stabilization could be mediated by CHP1, which suppressed the proliferation of cancer cells and the expression of angiogenic factors in the cells leading to inhibition of angiogenesis.

4. Discussion

We identified CHP1 as a new biologically relevant target protein of LW6 by phage display biopanning. A number of chemical, biophysical, and biological validations of the binding of LW6 to CHP1 were conducted; these strongly supported that the interaction of LW6 with CHP1 is relevant for its biological activity. The binding specificity of LW6 to CHP1 and their Ca^{2+}-dependent binding patterns were deciphered by phage binding assay and SPR analysis. Furthermore, to investigate the interaction of LW6 with CHP1 in

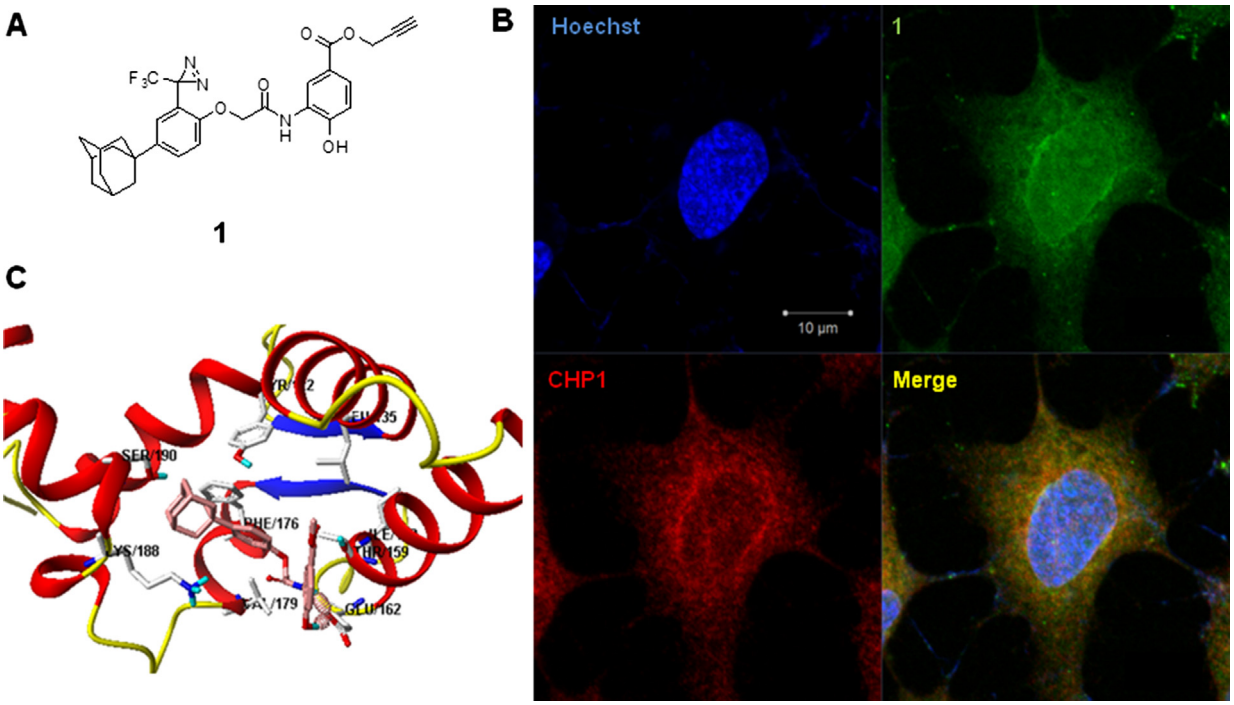

Fig. 3. Cellular localization of LW6 and the binding mode between LW6 and CHP1. (A) Chemical structure of photo-activatable and clickable probe 1. (B) Localization of probe 1 (3 μM, green) was detected via the click reaction using azide-linked Alexa Flour-488 in HUH7 cells. Nuclei (blue) were stained with Hoechst and CHP1 (red) was selectively stained with a CHP1 antibody and rabbit Alexa Flour-594. (C) Docking model of LW6 in the C-terminal CHP1 domain of the complex. (For interpretation of the references to colour in this figure legend, the reader is referred to the web version of this article.)

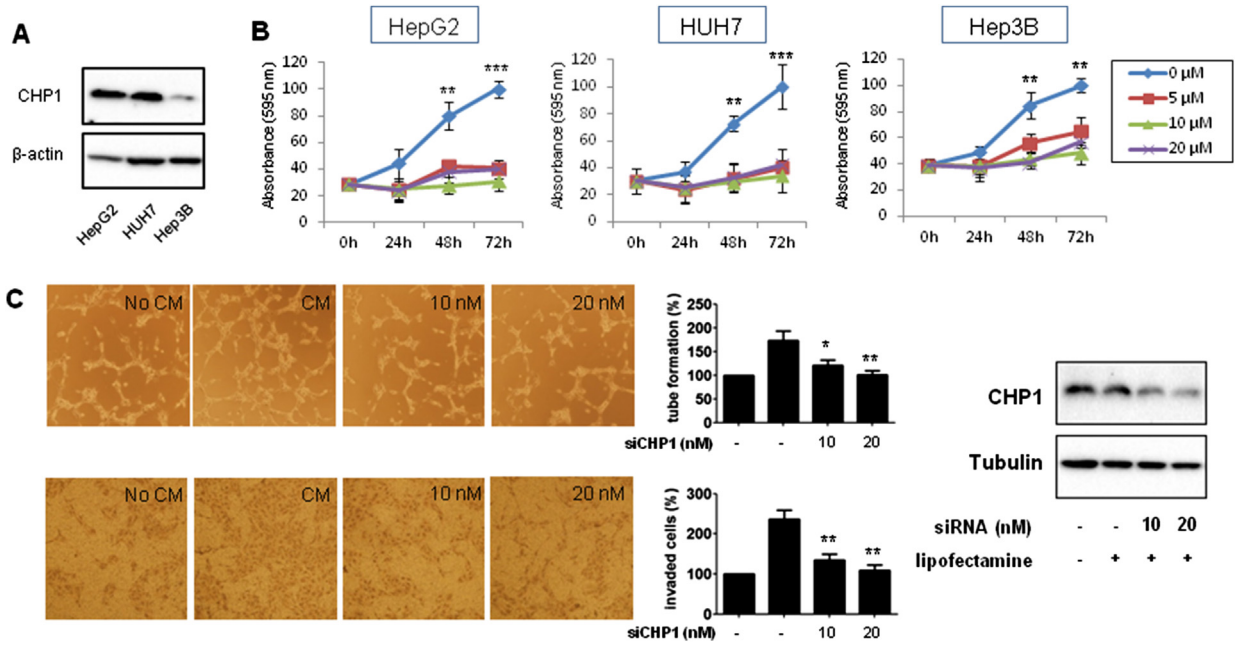

Fig. 4. Biological activity of LW6 and the effect of CHP1 on angiogenesis were validated. (A) CHP1 expression levels were detected by immunoblot analysis in HepG2, HUH7, and Hep3B cell lines. Among them, the expression level of CHP1 of HepG2 and HUH7 cells was higher than that of Hep3B. (B) To elucidate the effect of LW6 in various cell lines according to genetic background, the anti-proliferative effect of LW6 was determined by MTT assay. LW6 was treated for 24, 48 and 72 h at concentrations of 5–20 μM. CHP1-overexpressed cell lines, HepG2 and HUH7, were more susceptible to LW6 compared to Hep3B expressing CHP1. $^{**}p < 0.01$, versus control. (C) CHP1 knockdown by 10 and 20 nM of siRNA treatment was confirmed by immunoblot in HepG2 cells. Conditioned media from HepG2 cells was concentrated by microcon and applied onto HUVECs for in vitro angiogenesis assays.

live cells, we utilized both click chemistry and photoaffinity labeling. We noticed that it was not sufficient to detect localization of LW6 with fluorescence in the presence of CHP1 antibody when the compound harboring click conjugation alone was used, likely because the interaction between LW6 and CHP1 could be reversible and the CHP1 antibody might interfere with their interaction. Therefore, for target validation we applied photoactive covalent conjugation to the live cells as well as cell lysates, which can make it easier to detect the interaction between a compound and its target protein even though their binding might be reversible. As a result, CHP1 was shown to co-localize with a LW6 derived chemical probe harboring a photoaffinity moiety and a clickable tag in the cells. Next, relationship between CHP1 and angiogenesis was addressed by knockdown experiment. Interestingly, depletion of CHP1 moderately decreased HIF-1α stability, but did not affect VHL level (Figs. S3 and S4). This result indicated that inhibitory effect of LW6 on HIF-1α might be partially mediated by CHP1 perturbation in the VHL-independent manner. Notably, some proteins had been recently reported as VHL-independent HIF-1α regulators [21,22]. Accordingly, detailed mechanism of how CHP1 regulates HIF-1α stability will be our next agenda for exploration. In addition to CHP1, CaM was also identified as a target candidate of LW6 in phage display. We demonstrated the better affinity of LW6-CaM than LW6-CHP1 binding by phage binding assay and BIAcore/SPR. The K_D of LW6-CaM with Ca^{2+} was 3.61×10^{-7} M, which is lower than that of LW6-CHP1 with Ca^{2+}. CaM was found to share the homologous regions (Glu128 and Phe142) with CHP1 (Glu162 and Phe174), which provide strong binding affinity to LW6-CHP1 through hydrophobic and polar interactions as described above. Accordingly, following investigation on binding moiety of LW6 to calcium binding proteins will provide better structural information for developing drug candidates targeting cancer.

In summary, LW6, a HIF-1α inhibitor, acts as a CHP1 antagonist, which eventually results in suppression of tumor angiogenesis. This presents CHP1 as a new therapeutic target for perturbation of HIF-1α mediated angiogenesis. In addition, LW6 could be a new chemical scaffold for analysis of the underlying mechanisms in this process, having a "one-drug, multiple targets; single pharmacological effect" against tumor inhibition.

Conflict of interest

None declared.

Acknowledgments

This study was partly supported by grants from the National Research Foundation of Korea funded by the Korean Government (2010-0017984, 2012M3A9D1054520, 2014R1A2A2A01005455), the Translational Research Center for Protein Function Control, KRF (2009–0083522) and the Brain Korea 21 Plus Project, Republic of Korea.

Transparency document

The transparency document associated with this article can be found in the online version at http://dx.doi.org/10.1016/j.bbrc.2015.01.031.

Appendix A. Supplementary data

Supplementary data related to this article can be found at http://dx.doi.org/10.1016/j.bbrc.2015.01.031.

References

[1] J. Pouyssegur, F. Dayan, N.M. Mazure, Hypoxia signalling in cancer and approaches to enforce tumour regression, Nature 441 (2006) 437–443.
[2] K. Lee, H. Zhang, D.Z. Qian, S. Rey, J.O. Liu, G.L. Semenza, Acriflavine inhibits HIF-1 dimerization, tumor growth, and vascularization, Proc. Natl. Acad. Sci. U. S. A. 106 (2009) 17910–17915.
[3] G. Melillo, Inhibiting hypoxia-inducible factor 1 for cancer therapy, Mol. Cancer Res. 4 (2006) 601–605.

[4] G.L. Semenza, Evaluation of HIF-1 inhibitors as anticancer agents, Drug Discov. Today 12 (2007) 853–859.
[5] S.S. Syed Alwi, B.E. Cavell, U. Telang, M.E. Morris, B.M. Parry, G. Packham, In vivo modulation of 4E binding protein 1 (4E-BP1) phosphorylation by watercress: a pilot study, Br. J. Nutr. 104 (2010) 1288–1296.
[6] G.L. Semenza, Targeting HIF-1 for cancer therapy, Nat. Rev. Cancer 3 (2003) 721–732.
[7] K. Lee, J.E. Kang, S.K. Park, Y. Jin, K.S. Chung, H.M. Kim, M.R. Kang, M.K. Lee, K.B. Song, E.G. Yang, J.J. Lee, M. Won, LW6, a novel HIF-1 inhibitor, promotes proteasomal degradation of HIF-1alpha via upregulation of VHL in a colon cancer cell line, Biochem. Pharmacol. 80 (2010) 982–989.
[8] K. Lee, H.S. Ban, R. Naik, Y.S. Hong, S. Son, B.K. Kim, Y. Xia, K.B. Song, H.S. Lee, M. Won, Identification of malate dehydrogenase 2 as a target protein of the HIF-1 inhibitor LW6 using chemical probes, Angew. Chem. Int. Ed. Engl. 52 (2013) 10286–10289.
[9] P.P. Sche, K.M. McKenzie, J.D. White, D.J. Austin, Display cloning: functional identification of natural product receptors using cDNA-phage display, Chem. Biol. 6 (1999) 707–716.
[10] P. Imming, C. Sinning, A. Meyer, Drugs, their targets and the nature and number of drug targets, Nat. Rev. Drug Discov. 5 (2006) 821–834.
[11] N. Mine, S. Yamamoto, N. Saito, S. Yamazaki, C. Suda, M. Ishigaki, D.W. Kufe, D.D. Von Hoff, T. Kawabe, CBP501-calmodulin binding contributes to sensitizing tumor cells to cisplatin and bleomycin, Mol. Cancer Ther. 10 (2011) 1929–1938.
[12] G.I. Shapiro, R. Tibes, M.S. Gordon, B.Y. Wong, J.P. Eder, M.J. Borad, D.S. Mendelson, N.J. Vogelzang, B.R. Bastos, G.J. Weiss, C. Fernandez, W. Sutherland, H. Sato, W.E. Pierceall, D. Weaver, S. Slough, E. Wasserman, D.W. Kufe, D. Von Hoff, T. Kawabe, S. Sharma, Phase I studies of CBP501, a G2 checkpoint abrogator, as monotherapy and in combination with cisplatin in patients with advanced solid tumors, Clin. Cancer Res. 17 (2011) 3431–3442.
[13] H.J. Jung, J.H. Kim, J.S. Shim, H.J. Kwon, A novel Ca2+/calmodulin antagonist HBC inhibits angiogenesis and down-regulates hypoxia-inducible factor, J. Biol. Chem. 285 (2010) 25867–25874.
[14] A. Villalobo, I. Garcia-Palmero, S.R. Stateva, K. Jellali, Targeting the calmodulin-regulated ErbB/Grb7 signaling axis in cancer therapy, J. Pharm. Pharm. Sci. 16 (2013) 177–189.
[15] J.J. Provost, M.A. Wallert, Inside out: targeting NHE1 as an intracellular and extracellular regulator of cancer progression, Chem. Biol. Drug Des. 81 (2013) 85–101.
[16] S. Nakayama, R.H. Kretsinger, Evolution of the EF-hand family of proteins, Annu Rev. Biophys. Biomol. Struct. 23 (1994) 473–507.
[17] M. Mishima, S. Wakabayashi, C. Kojima, Solution structure of the cytoplasmic region of Na+/H+ exchanger 1 complexed with essential cofactor calcineurin B homologous protein 1, J. Biol. Chem. 282 (2007) 2741–2751.
[18] L. Dubinsky, B.P. Krom, M.M. Meijler, Diazirine based photoaffinity labeling, Bioorg. Med. Chem. 20 (2012) 554–570.
[19] A.N. Jain, Surflex-Dock 2.1: robust performance from ligand energetic modeling, ring flexibility, and knowledge-based search, J. Comput Aided Mol. Des. 21 (2007) 281–306.
[20] A. Matsuyama, R. Arai, Y. Yashiroda, A. Shirai, A. Kamata, S. Sekido, Y. Kobayashi, A. Hashimoto, M. Hamamoto, Y. Hiraoka, S. Horinouchi, M. Yoshida, ORFeome cloning and global analysis of protein localization in the fission yeast *Schizosaccharomyces pombe*, Nat. Biotechnol. 24 (2006) 841–847.
[21] J. Zhou, R. Kohl, B. Herr, R. Frank, B. Brune, Calpain mediates a von Hippel-Lindau protein-independent destruction of hypoxia-inducible factor-1alpha, Mol. Biol. Cell. 17 (2006) 1549–1558.
[22] D. Zhang, J. Li, M. Costa, J. Gao, C. Huang, JNK1 mediates degradation HIF-1alpha by a VHL-independent mechanism that involves the chaperones Hsp90/Hsp70, Cancer Res. 70 (2010) 813–823.